Accepted Manuscript

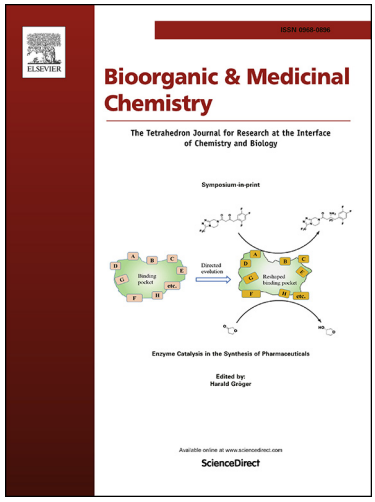

Development of 13*H*-benzo[*f*]chromeno[4,3-*b*][1,7]naphthyridines and Their Salts as Potent Cytotoxic Agents and Topoisomerase I/ IIα Inhibitors

Sateesh Kumar Arepalli, Chaerim Lee, Seongrak Sim, Kiho Lee, Hyunji Jo, Kyu-Yeon Jun, Youngjoo Kwon, Jong-Soon Kang, Jae-Kyung Jung, Heesoon Lee

PII: S0968-0896(18)31291-4
DOI: https://doi.org/10.1016/j.bmc.2018.09.019
Reference: BMC 14544

To appear in: *Bioorganic & Medicinal Chemistry*

Received Date: 16 July 2018
Revised Date: 27 August 2018
Accepted Date: 17 September 2018

Please cite this article as: Arepalli, S.K., Lee, C., Sim, S., Lee, K., Jo, H., Jun, K-Y., Kwon, Y., Kang, J-S., Jung, J-K., Lee, H., Development of 13*H*-benzo[*f*]chromeno[4,3-*b*][1,7]naphthyridines and Their Salts as Potent Cytotoxic Agents and Topoisomerase I/ IIα Inhibitors, *Bioorganic & Medicinal Chemistry* (2018), doi: https://doi.org/10.1016/j.bmc.2018.09.019

Development of 13*H*-benzo[*f*]chromeno[4,3-*b*][1,7]naphthyridines and Their Salts as Potent Cytotoxic Agents and Topoisomerase I/ IIα Inhibitors

Sateesh Kumar Arepalli[a], Chaerim Lee[a], Seongrak Sim[a], Kiho Lee[b], Hyunji Jo[c], Kyu-Yeon Jun[c], Youngjoo Kwon[c], Jong-Soon Kang[d], Jae-Kyung Jung[a] and Heesoon Lee[a]*

[a]*College of Pharmacy, Chungbuk National University, Chungbuk 28160, Republic of Korea*

[b]*College of Pharmacy, Korea University, Sejong 30019, Republic of Korea*

[c]*College of Pharmacy, Ewha Womans University, Seoul 03760, Republic of Korea*

[d]*Korea Research institute of Bioscience and Biotechnology, Chungbuk 28116, Republic of Korea*

* Corresponding author. Tel.: +82-43-261-2811; fax: +82-43-268-2732; e-mail: medchem@chungbuk.ac.kr (H. Lee)

Abstract

A novel series of 35 angularly fused pentacyclic 13*H*-benzo[*f*]chromeno[4,3-*b*][1,7]naphthyridines and 13*H*-benzo[*f*]chromeno[4,3-b][1,7]naphthyridin-5-ium chlorides were designed and synthesized. Their cytotoxic activities were investigated against six human cancer cell lines (NCIH23, HCT15, NUGC-3, ACHN, PC-3, and MDA-MB-231). Among all screened compounds; **28**, **30**, **34**, **35**, **46**, **48**, **52**, and **53** compounds exhibited potential cytotoxic activities against all tested human cancer cell lines. Further, these potent lead cytotoxic agents were evaluated against human Topoisomerase I and IIα inhibition. Among them, the compound **48** exhibited dual Topoisomerase I and IIα inhibition especially at 20 μM concentrations the compound **48** exhibited 1.25 times more potent Topoisomerase IIα inhibitory activity (38.3%) than the reference drug etoposide (30.6 %). The compound **52** also exhibited excellent (88.4 %) topoisomerase I inhibition than the reference drug camptothecin (66.7 %) at 100 μM concentrations. Molecular docking studies of the compounds **48** and **52** with topo I discovered that they both intercalated into the DNA single-strand cleavage site where the compound **48** have van der Waals interactions with residues Arg364, Pro431, and Asn722 whilst the compound **52** have with Arg364, Thr718, and Asn722 residues. Both the compounds **48** and **52** have π- π stacking interactions with the stacked DNA bases. The docking studies of the compound **48** with topo IIα explored that it was bound to the topo IIα DNA cleavage site where etoposide was situated. The benzo[*f*]chromeno[4,3-*b*][1,7]naphthyridine ring of the compound **48** was stacked between the DNA bases of the cleavage site with π- π stacking interactions and there were no hydrogen bond interactions with topo IIα.

Key words

13*H*-benzo[*f*]chromeno[4,3-*b*][1,7]naphthyridines; Dual human Topoisomerase I and IIα inhibition; Cytotoxicity; Molecular docking; Imino Diels-Alder reaction

1. Introduction

Human topoisomerases are essential nuclear enzymes that play a vital role in DNA topology by releasing torsional strain induced during replication, transcription, recombination, mitosis and chromatin remodeling processes.[1-5] These enzymes are important target for a number of clinically used anticancer drugs owing to their over-expression in cancer cells. Two types of human topoisomerases existed namely, type I topoisomerase (Topo I) and type II topoisomerase (Topo II). Human Topo I enzyme catalyzes the formation of DNA single-strand breaks in absence of binding of ATP and Mg (II) and then rejoined. Topo II enzyme acts as homodimer which engender double strand breaks with binding of ATP and Mg (II).[5-6] Further two isoforms of topo II characterized namely α and β,[6-7] but expression of α isoforms is firmly reliant on cellular proliferation status, though the β isoform is expressed during the cell cycle.[8] Camptothecin analogues such as topotecan, irinotecan and belotecan were used topo I as central target for treatment of colon cancer. [9-10] Additionally topo I expression is discernible in ovarian cancer, prostate cancer, and malignant lymphoma. Doxorubicin, etoposide, daunorubicin, teniposide, idarubicin, mitoxantrone and epipodophyllotoxins were used topo II as main target for treatment of different malignancies[11-21] since topo II is also expressed in breast cancer, ovarian cancer and malignant lymphoma. Most of the reported topo inhibitors displayed selective

inhibition toward topo I or topo II but scarce compounds available for dual topo I and topo II inhibition.[22-26] Therefore, an agent exhibits both topo I and topo II inhibition as dual topo inhibitor has received greater attention due to broader anticancer spectrum and advantages. [27-28] In recent times, researchers focused to design and develop dual top I & II inhibitors with potential cytotoxicities.[29-36] In this regard as part of developing novel potential anticancer agents, our group also developed novel 1,8-diazaanthraquinone derivatives and 1,3-diphenylbenzo[*f*][1,7]naphthyridines as human topoisomerase IIα inhibitors with potential cytotoxicities against several cancer cell lines.[37-38] Besides, the chromene moiety is an important ubiquitous structural motif in a wide range of biologically active compounds and natural products.[39] Chromene fused heterocycles are also well known for their biological and pharmacological properties. For instance 6*H*-chromeno[4,3-*b*]quinolines and chromenopyridinones are act as potent HSP90 inhibitors,[40] anti-inflammatory and potent cytotoxic agents.[41-43] Angularly fused heterocycles (Fig. 1) such as chromeno[4,3-*b*]pyridines, [44,45] indeno[1,2-b]pyridines,[46] benzo[*a*]phenazines,[47] benzofuro[3,2-*b*]pyridines,[48,49] dihydrothieno[2,3-*h*]quinolines,[50] dihydro-1,10-phenanthrolines[51] are acknowledged for their non-intercalative topo I and II dual catalytic inhibition properties. The preamble of angular fused heterocycles with conformational rigidity on topo I/ IIα-targeting compounds fit further efficiently into the active site of enzymes and work as an intercalator in the enzyme−DNA complex.[52-55] Since rigid molecules are typically assumed to have less conformational entropy and can be built into the active site of a receptor. On the basis of these considerations, in this study we have designed and synthesized 35 angularly fused and pentacyclic 13*H*-benzo[*f*]chromeno[4,3-*b*][1,7]naphthyridines (**21**-**39**) and 13*H*-benzo[*f*]chromeno[4,3-*b*][1,7]naphthyridin-5-ium chlorides (**40**-**56**) as shown in Scheme 1. The synthesized compounds

were evaluated for cytotoxic activities against six human cancer cell lines, topo I and IIα inhibitory activities and also carried out docking studies for the potent lead compounds.

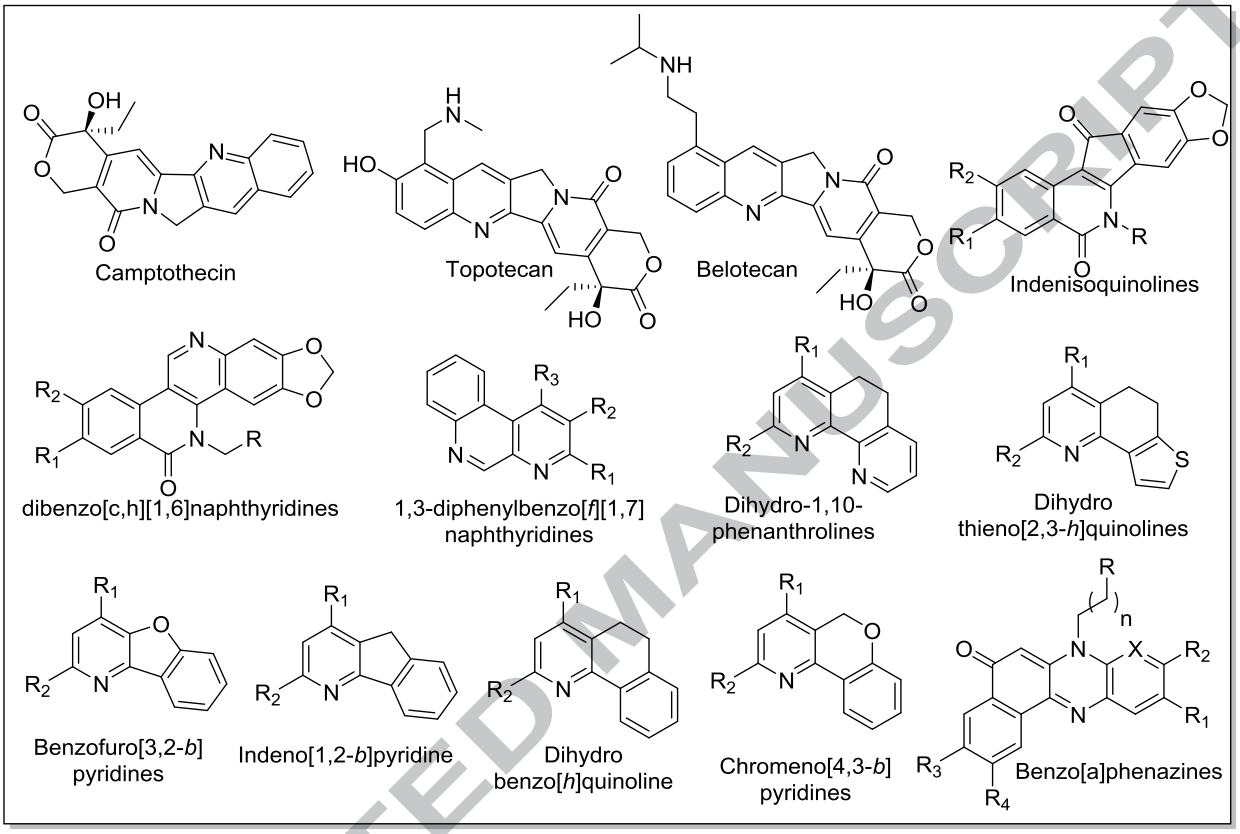

Fig 1. Representative angularly fused heterocycles as topo I/IIα inhibitors

2. Results and discussion

2.1. Chemistry

We initially envisaged the synthesis of 13*H*-benzo[*f*]chromeno[4,3-*b*][1,7]naphthyridines as a part of our continuous interest in the synthesis of medicinally and biologically important heterocyclic scaffolds[56-61] collectively with an urge to develop an operationally simple and best synthetic route for desired molecules unlike multistep synthesis for angularly fused heterocycles.

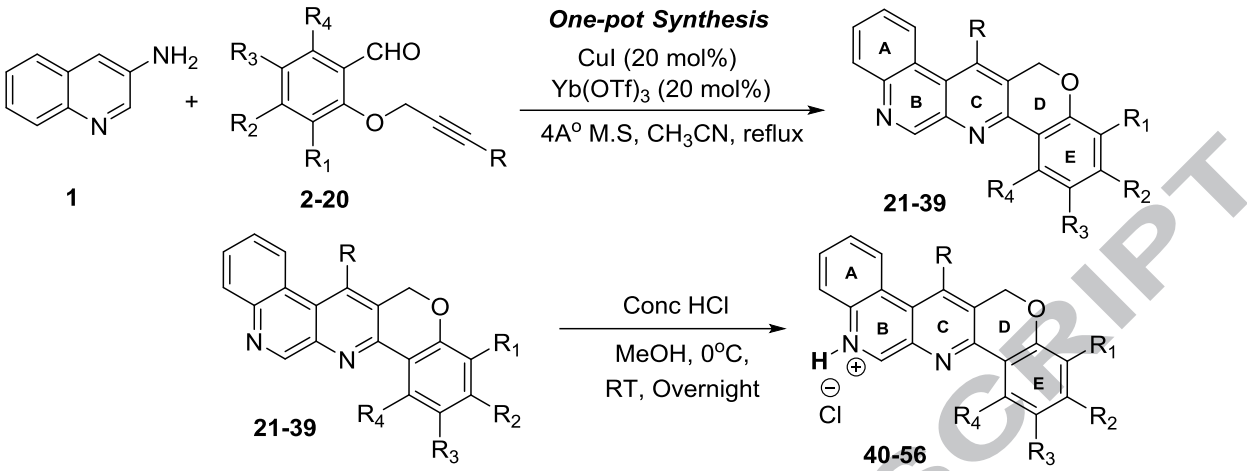

Scheme 1. General synthetic one-pot method for the synthesis of 13*H*-benzo[*f*]chromeno[4,3-*b*][1,7]naphthyridines and 13H-benzo[*f*]chromeno[4,3-*b*][1,7]naphthyridin-5-ium chlorides.

Hence we developed one-pot, atom-economic and regioselective intramolecular imino Diels-Alder reaction method for 13*H*-benzo[*f*]chromeno[4,3-*b*][1,7]naphthyridines **21-39** as shown in Scheme 1. After screened different reaction parameters, the reaction condition for the synthesis of 13*H*-benzo[*f*]chromeno[4,3-*b*][1,7]naphthyridines **21-39** found to involve 20 mol% CuI, 20 mol% $Yb(OTf)_3$, 0.5 equiv. of 4 Å Molecular sieves in 5–10 mL of CH_3CN at reflux temperature afford the desired intramolecular imino Diels-Alder products **21-39** as shown in scheme 1. The structures of all synthesized products were unambiguously confirmed by ^1H and ^{13}C NMR spectra. Subsequently, the salt formation was accomplished by suspending the corresponding 13*H*-benzo[*f*]chromeno[4,3-*b*][1,7]naphthyridines in methanol and addition of Conc. HCl at 0°C then stir 1 h and followed by stir at room temperature for overnight. The hydrochloride salts of 13*H*-benzo[*f*]chromeno[4,3-*b*][1,7]naphthyridines **40-56** were obtained in almost quantitative yields by concentration of reaction mixture under reduced pressure. These compounds structures

(Scheme 1 and Table 1) were also confirmed by ^{1}H and ^{13}C NMR spectra. The compounds **40-56** were evidently distinguishable by ^{1}H and ^{13}C NMR from the compounds **21-39**. To explain the characteristic peak difference among them; for instance in the ^{1}H NMR spectra, the compound **30** displayed characteristic singlet peaks at δ 9.47 and 5.09 ppm respectively while its hydrochloride salt compound **48** shown downfield singlet peaks at δ 10.00 and 5.19 ppm respectively (Table S3). Similarly the compound **34** displayed characteristic singlet peaks at δ 9.46, 9.02 and 5.54 ppm respectively whereas its salt derivative **52** shown downfield singlet peaks at δ 10.08, 9.32 and 5.69 ppm respectively (Table S4).

2.2.1. Cytotoxic activity

Having 35 novel chemical libraries in hand, we started evaluation against six different human cancer cell lines. The utilized human cancer cell lines in this study were lung cancer cell line (NCIH23), colon cancer cell line (HCT15), gastric cancer cell line (NUCG-3), renal cancer cell line (ACHN), prostate cancer cell line (PC-3), and breast cancer cell line (MDA-MB-231) with reference drug doxorubicin (ADR) as shown in Table 1 and Fig. 3, S1 & S2. The growth inhibitory activity (GI_{50}) is expressed as micromolar concentration as shown in Table 1 and these values are taken as a mean from three experiments and correspond to the agent's concentration causing a 50% decrease in net cell growth. Among all tested chemical libraries, 8 compounds **28**, **30**, **34**, **35**, **46**, **48**, **52**, and **53** displayed potential cytotoxicities with GI_{50} values less than 10μM range in all tested human cancer cell lines as shown in Table 1. Amongst the compounds **28, 35, 46**, **48**, **52**, and **53** exhibited strong inhibition against all human cancer cell lines. This phenomenon also supported by the analysis of cell viabilities at 10μM range concentrations (Fig. 3) and which is also established to be most consistent with GI_{50} values estimated in this study

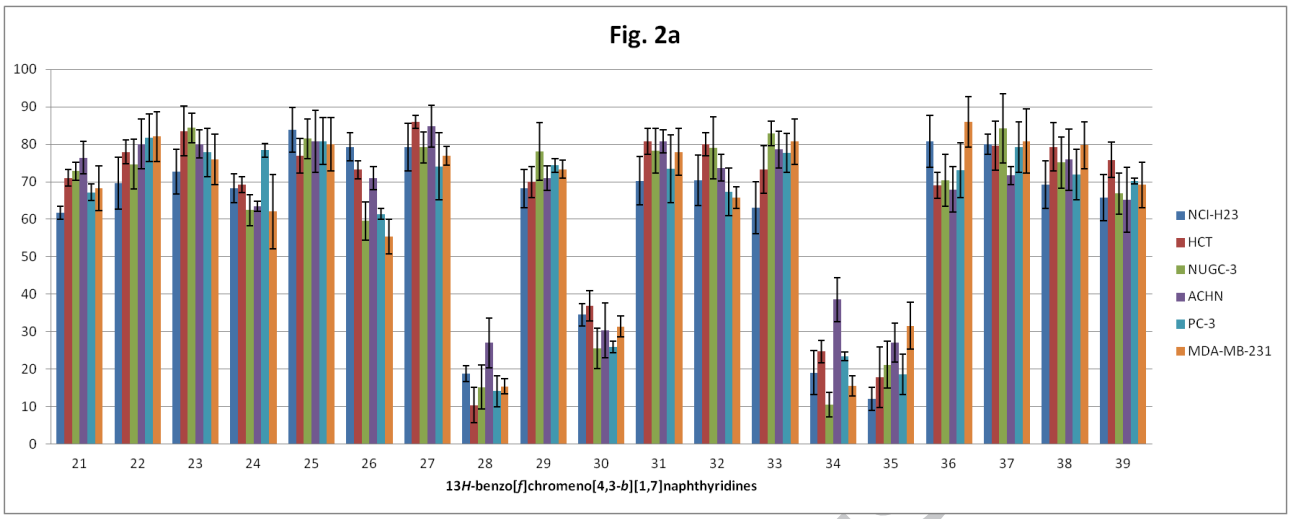

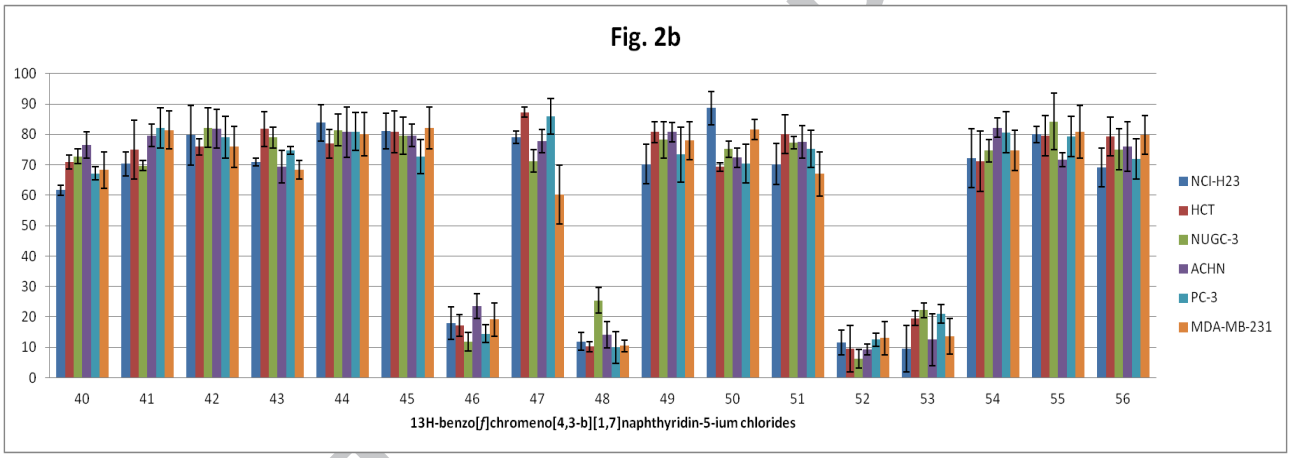

Fig. 2. The cell viabilities of 13*H*-benzo[*f*]chromeno[4,3-*b*][1,7]naphthyridines (**2a**) and 13H-benzo[*f*]chromeno[4,3-*b*][1,7]naphthyridin-5-ium chlorides (**2b**) at 10 μM concentration on human lung cancer (NCIH23), colon cancer (HCT15), gastric cancer (NUCG-3), renal cancer (ACHN), prostate cancer (PC-3), and breast cancer (MDA-MB-231) cell lines.

(Fig. S1 & S2**)**. After synthesize different substitutions on core motifs of benzo[*f*]chromeno[4,3-*b*][1,7]naphthyridines and benzo[*f*]chromeno[4,3-*b*][1,7]naphthyridin-5-ium chlorides, we noticed the substituents on C and E rings (Scheme 1) were crucial to explain structure activity relationship (SAR). When methyl substituent on C ring with different substitution like –I and +I

groups on E ring (compounds **21-29**) did not exhibit considerable cytotoxic activities against all tested human cancer cell lines except the compound **28** which is having methoxy substituent (+M group) on E ring. It was exhibited significant cytotoxic activities against all six human cancer cell lines in the range of GI_{50}: 1.520-2.622 μM as shown in Table 1. Interestingly, when we screened the scaffolds with no methyl substitution on C ring and –I groups such as –F and –Cl on E ring exhibited significant cytotoxicities against all human cancer cell lines. For example compound **34** (GI_{50}: 1.847-3.205 μM) and compound **35** (GI_{50}: 1.185-2.716 μM) were exhibited significant cytotoxicities against all human cancer cell lines. We also noted that tolyl group on C ring with no substitution on E ring (compound **30**) exhibited considerable cytotoxic activities against colon (HCT15), gastric (NUCG-3), renal (ACHN), prostate (PC-3), and breast cancer cell lines in the range of GI_{50}: 2.398-5.024 μM. After screening of 13*H*-benzo[*f*]chromeno[4,3-*b*][1,7]naphthyridines (**21-39**), we observed that only four compounds exhibited moderate to considerable cytotoxicities but remaining compounds did not exhibit even nominal cytotoxicities against all tested human cancer cell lines due to their partial solubilities in DMSO media. Hence in order to improve the solubilities of **21-39**, 13*H*-benzo[*f*]chromeno[4,3-b][1,7]naphthyridin-5-ium chlorides (**40-56**) were synthesized and evaluated against all six human cancer cell lines as shown in Table 1. As anticipated the compounds **40-56** have displayed strong cytotoxicities against all screened human cancer cell lines than the 13*H*-benzo[*f*]chromeno[4,3-*b*][1,7]naphthyridines (**21-39**). Among them, the compounds **46**, **48**, **52** and **53** were exhibited higher cytotoxicities against all tested human cancer cell lines in the range of GI_{50}: 0.900-2.699 μM. In order to explain the potential cytotoxic activities of all compounds **21-39** and **40-56** toward each human cancer cell lines, for lung cancer cell line (NCIH23) compound **53** exhibited higher cytotoxicity (GI_{50}: 0.900 μM) than the remaining compounds.

Table 1. *In vitro* cytotoxic activities of 13*H*-benzo[*f*]chromeno[4,3-*b*][1,7]naphthyridines and 13H-benzo[*f*]chromeno[4,3-b][1,7]naphthyridin-5-ium chlorides on different human cancer cell lines

Compounds (21-39)[b] & (40-56)	Human Cancer cell lines GI_{50} (μM)[a]					
	NCIH23 (Lung)	**HCT15 (Colon)**	**NUGC-3 (Gastric)**	**ACHN (Renal)**	**PC-3 (Prostate)**	**MDA-MB-231 (Breast)**
ADR (Reference)	0.090	0.077	0.086	0.080	0.076	0.068
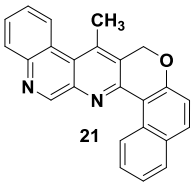 **21**	>10	>10	>10	>10	>10	>10
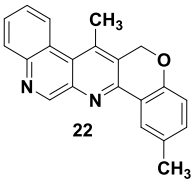 **22**	>10	>10	>10	>10	>10	>10
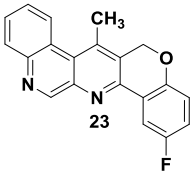 **23**	>10	>10	>10	>10	>10	>10
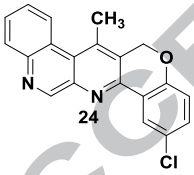 **24**	>10	>10	>10	>10	>10	>10
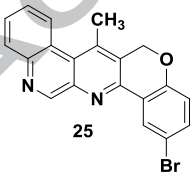 **25**	>10	>10	>10	>10	>10	>10

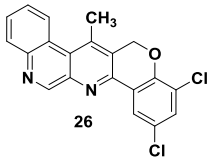 26	>10	>10	>10	>10	>10	>10
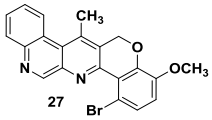 27	>10	>10	>10	>10	>10	>10
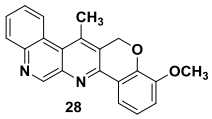 28	**1.557**	**1.787**	**2.622**	**2.191**	**1.607**	**1.520**
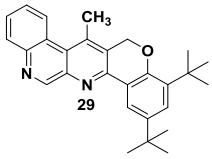 29	>10	>10	>10	>10	>10	>10
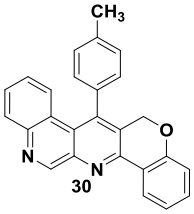 30	>10	**4.230**	**3.852**	**2.398**	**5.024**	**5.616**
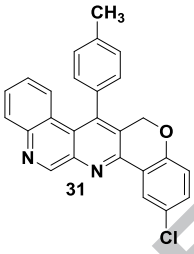 31	>10	>10	>10	>10	>10	>10
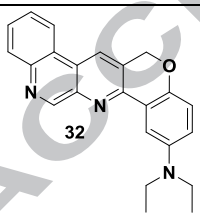 32	>10	>10	>10	>10	>10	>10
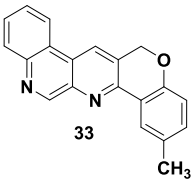 33	>10	>10	>10	>10	>10	>10

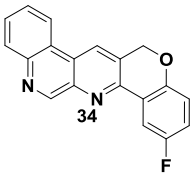	**1.867**	**2.195**	**1.847**	**3.205**	**2.794**	**2.204**
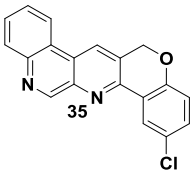	**1.185**	**1.567**	**2.208**	**2.559**	**1.496**	**2.716**
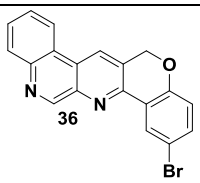	>10	>10	>10	>10	>10	>10
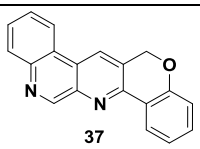	>10	>10	>10	>10	>10	>10
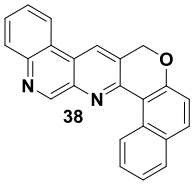	>10	>10	>10	>10	>10	>10
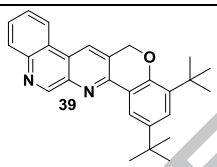	>10	>10	>10	>10	>10	>10
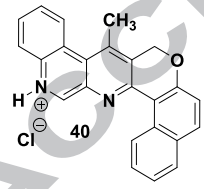	>10	>10	>10	>10	>10	>10
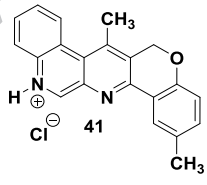	>10	>10	>10	>10	>10	>10

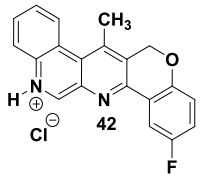	>10	>10	>10	>10	>10	>10
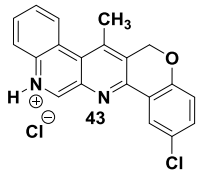	>10	>10	>10	>10	>10	>10
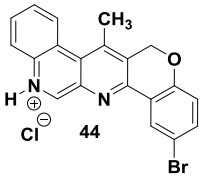	>10	>10	>10	>10	>10	>10
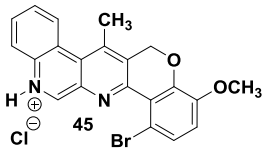	>10	>10	>10	>10	>10	>10
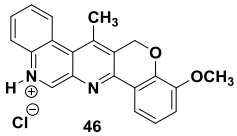	**2.392**	**1.289**	**1.556**	**2.008**	**2.059**	**1.670**
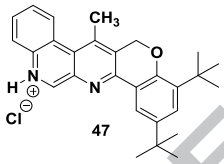	>10	>10	>10	>10	>10	>10
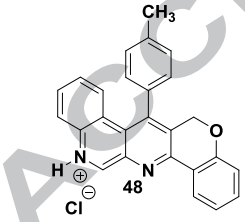	**2.059**	**2.715**	**2.699**	**2.284**	**1.528**	**1.787**

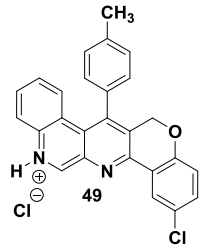 49	>10	>10	>10	>10	>10	>10
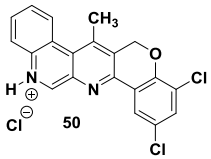 50	>10	>10	>10	>10	>10	>10
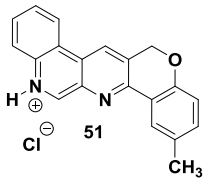 51	>10	>10	>10	>10	>10	>10
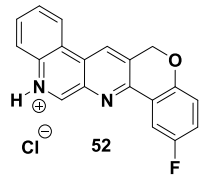 52	**1.026**	**1.564**	**1.371**	**1.004**	**1.273**	**1.234**
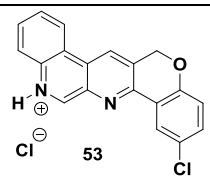 53	**0.900**	**1.089**	**1.162**	**1.079**	**1.671**	**1.046**
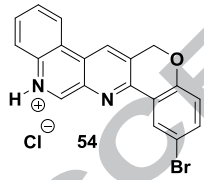 54	>10	>10	>10	>10	>10	>10
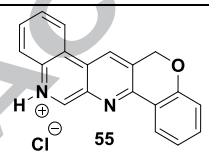 55	>10	>10	>10	>10	>10	>10
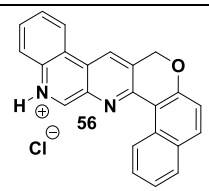 56	>10	>10	>10	>10	>10	>10

[a]GI_{50} values are taken as a mean from three experiments and correspond to the agent's concentration causing a 50% decrease in net cell growth. [b]These derivatives have partial solubility

For colon cancer cell line (HCT15) compounds **53** and **46** exhibited higher cytotoxicities (GI_{50}: 1.089 & 1.289 μM respectively) than other compounds. For gastric cancer cell line (NUGC-3) compounds **53** and **52** exhibited higher cytotoxicities (GI_{50}: 1.162 & 1.371 μM respectively). For renal cancer cell line (ACHN) compounds **52** and **53** exhibited higher cytotoxicities (GI_{50}: 1.004 & 1.079 μM respectively). For prostate cancer cell line (PC-3) compounds **52** and **35** exhibited higher cytotoxicities (GI_{50}: 1.273 & 1.496 μM respectively). For breast cancer cell line (MDA-MB-231) compounds **52** and **53** exhibited higher cytotoxicities (GI_{50}: 1.234 & 1.046 μM respectively). The cytotoxicity of these compounds on each human cancer cell line was also shown in Fig. S1 and Fig S2. To sum up the cytotoxic activities, 8 compounds such as **28**, **30**, **34**, **35**, **46**, **48**, **52**, and **53** demonstrated potential cytotoxic activities against all tested human cancer cell lines as shown in Table 1, Fig 3, S1 and S2. In particular, these compounds are more effective toward lung cancer (NCIH23) and prostate cancer (PC-3) cell lines than other tested human cancer cell lines.

2.2.2. Topoisomerase I & IIα inhibition

Subsequent to the discovery of lead 8 cytotoxic agents (**28**, **30**, **34**, **35**, **46**, **48**, **52**, and **53**), we targeted to evaluate the effect of these compounds on human DNA topo I and IIα with relaxing assay using super coiled plasmid DNA. Camptothecin and etoposide are used as references for topo I and II inhibitors respectively. The inhibitory activities of these compounds on topo I and IIα are shown in Fig. 3 & 4 and by using densitometry analysis and their quantified activities are listed in Table 2.

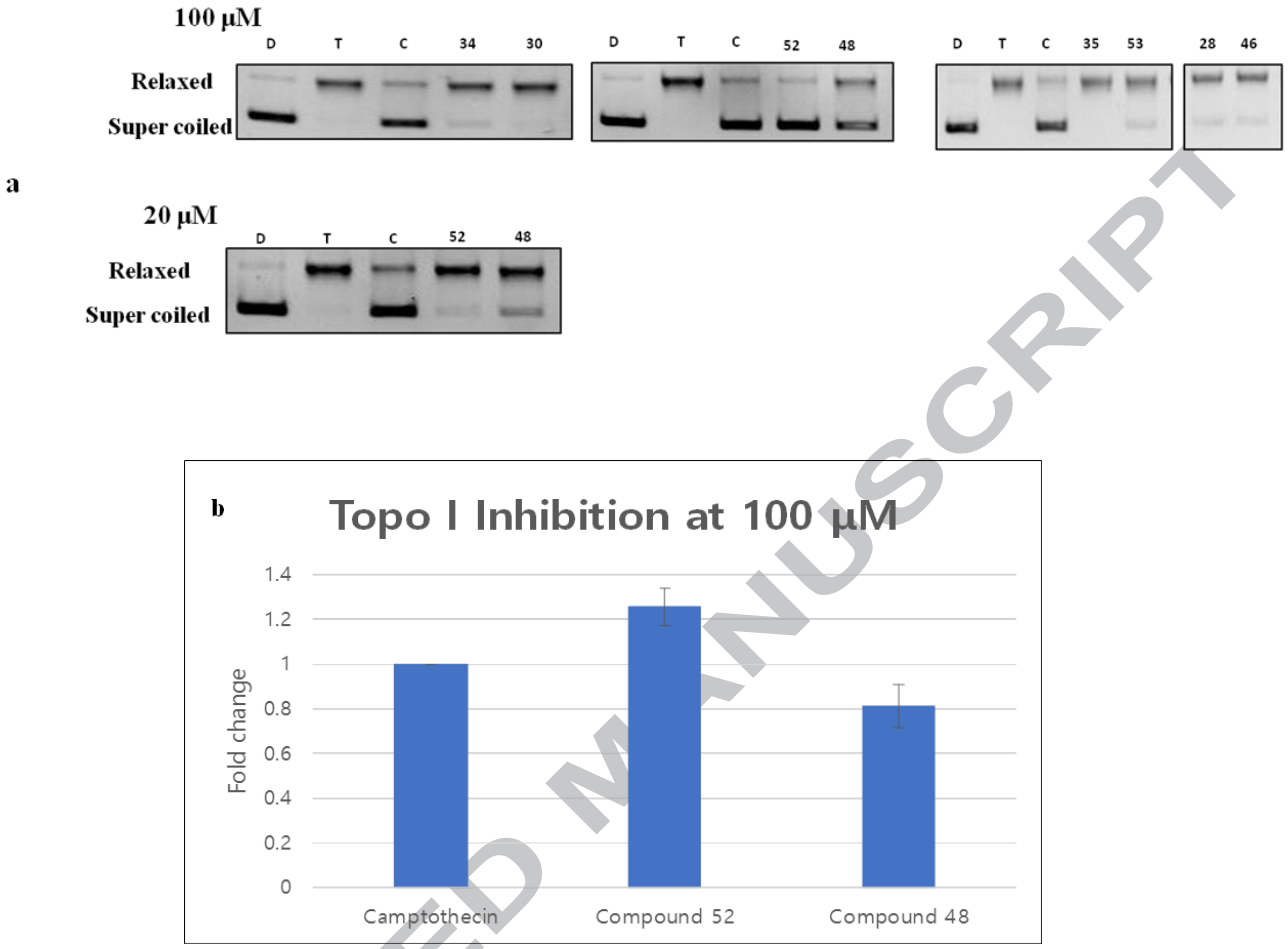

Fig. 3. (a) Human DNA topo I inhibitory activity of lead 13*H*-benzo[*f*]chromeno[4,3-*b*][1,7]naphthyridines and 13H-benzo[*f*]chromeno[4,3-b][1,7]naphthyridin-5-ium chlorides at the concentration of 100 µM and 20 µM. **Land D:** pBR322 DNA only; **lane T:** pBR322 DNA+ Topo I; **lane C:** pBR322 DNA+ Topo I + Camptothecin; **lane 34:** pBR322 DNA+ Topo I + compound 34; **lane 30:** pBR322 DNA+ Topo I + compound 30; **lane 52:** pBR322 DNA+ Topo I + compound 52; **lane 48:** pBR322 DNA+ Topo I + compound 48; **lane 53:** pBR322 DNA+ Topo I + compound 53; **lane 28:** pBR322 DNA+ Topo I + compound 28; **lane 46:** pBR322 DNA+ Topo I + compound 46. (b) Graphical representation of Topo I inhibition for the lead compounds at 100 µM concentrations.

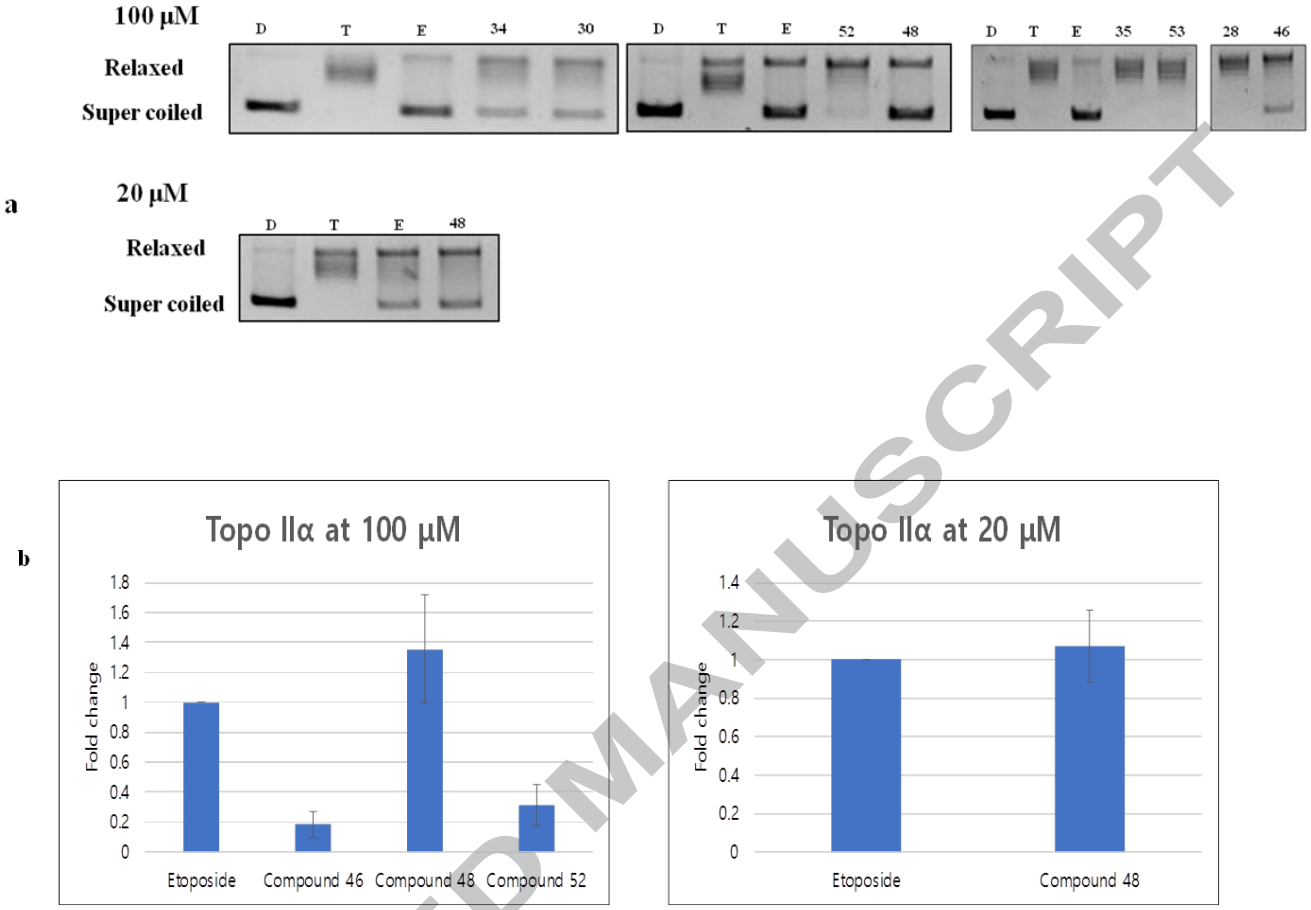

Fig. 4. (a) Human DNA topo IIα inhibitory activity of lead 13*H*-benzo[*f*]chromeno[4,3-*b*][1,7]naphthyridines and 13H-benzo[*f*]chromeno[4,3-b][1,7]naphthyridin-5-ium chlorides at the concentration of 100 µM and 20 µM. **Land D:** pBR322 DNA only; lane T: pBR322 DNA+ Topo II; **lane E:** pBR322 DNA+ Topo II + Etoposide; **lane 34:** pBR322 DNA+ Topo II + compound 34; **lane 30:** pBR322 DNA+ Topo II + compound 30; **lane 52:** pBR322 DNA+ Topo II + compound 52; lane 48: pBR322 DNA+ Topo II + compound 48; **lane 53:** pBR322 DNA+ Topo II + compound 53; **lane 28:** pBR322 DNA+ Topo II + compound 28; **lane 46:** pBR322 DNA+ Topo II + compound 46. (b) Graphical representation of Topo IIα inhibition for the lead compounds at 100 and 20 µM concentrations.

Table 2. Inhibitory activities of lead 13*H*-benzo[*f*]chromeno[4,3-*b*][1,7]naphthyridines and 13*H*-benzo[*f*]chromeno[4,3-b][1,7]naphthyridin-5-ium chlorides on human Topo I and IIα

Compounds	% Inhibition of Topo I		% Inhibition of Topo IIα	
	100μM	**20μM**	**100μM**	**20μM**
Camptothecin	66.7	44.4	NT[a]	NT[a]
Etoposide	NT[a]	NT[a]	70.4	30.6
28	14.4	NT[a]	0.0	NT[a]
30	3.0	NT[a]	14.9	NT[a]
34	7.0	NT[a]	14.5	NT[a]
35	1.7	NT[a]	0.0	NT[a]
46	10.2	NT[a]	23.5	NT[a]
48	57.2	11.1	69.8	38.3
52	88.4	4.2	12.2	NT[a]
53	12.3	NT[a]	0.0	NT[a]

[a]Not tested

When we screened the inhibitory activities of 13*H*-benzo[*f*]chromeno[4,3-*b*][1,7]naphthyridines against Topo I and IIα, initially we tested their activities at 100 μM concentration level. If they exhibited more than 30% inhibitory activities then we further tested at 20 μM concentration levels. Each experiment was performed with different concentrations with positive controls such as camptothecin for Topo I and etoposide for Topo IIα. Since the percentage of inhibition of Topo I and IIα are often dose-independent.[48, 62] 13*H*-benzo[*f*]chromeno[4,3-*b*][1,7]naphthyridines such as the compounds **28**, **30**, **34** and **35** exhibited 14.4%, 3.0%, 7.0%, and 1.7% nominal

inhibitory activities respectively on topo I at 100μM concentration level where as 13*H*-benzo[*f*]chromeno[4,3-*b*][1,7]naphthyridin-5-ium chlorides such as **46**, **48**, **53** and **52**compounds displayed 10.2%, 57.2%, 12.3% and 88.4% nominal to excellent inhibitory activities respectively on topo I at 100μM concentration level as shown in Table 2 and Fig 3a. Among all tested 8 compounds, the compound **52** exhibited excellent topo I inhibitory effect (88.4%) than the reference drug camptothecin (66.7 %) which is 1.32 times more strong topo I inhibition than the positive control camptothecin at 100μM concentration level as shown in Fig. 3 and Table 2. The compound **48** also exhibited moderate 57.2 % Topo I inhibitory effect at 100μM concentration level (Fig. 3a and Table 2). The compounds **48** and **52** also displayed 11.1% and 4.2% topo I inhibitory activities respectively at 20 μM concentration level (Fig. 3b and Table 2). We have also assessed the effect of 8 compounds on human DNA topo IIα (Table 2 and Fig. 3). The compounds **30**, **34, 46**, **48**, and **52** exhibited 14.9%, 14.5%, 23.5%, 69.8% and 12.2% topo IIα inhibitory activities respectively at 100μM concentration. Among them, the compound **48** exhibited almost similar (69.8%) topo IIα inhibitory activity with the reference drug etoposide (70.4%) at 100 μM concentrations but at 20 μM concentrations, the compound **48** exhibited excellent topo IIα inhibitory activity (38.3%) than the reference drug etoposide (30.6 %) which is 1.25 times more strong potent topo IIα inhibition than the reference drug etoposide. Topo I and IIα inhibition of 8 compounds indicated the fewer DNA breaks in gel (Fig 3 & 4) enlightening their potential cytotoxicities in human cancer cell lines which were in agreement with the cell viability and cytotoxic data (Table 1, Fig S1 & S2). Fig 3 & 4 and Table 2 summarized the topo I and IIα inhibitory activities of **28**, **30**, **34**, **35**, **46**, **48**, **52**, and **53** compounds; above all the compound **48** which contain tolyl group on C ring with no substituents on E ring exhibited excellent dual topo I and topo IIα inhibitory activities at 100 and 20 μM concentrations than the

positive controls camptothecin and etoposide respectively. The compound **52** which contain no substituent on C ring and –F substituent on E ring exhibited strong top I inhibitory than the positive control camptothecin at 100 μM concentration. The obtained results indicated that the compounds **48** and **52** were also found to have broad-spectrum cytotoxic activities against tested six human cancer cell lines (Table 1 and Fig. 2, S1 & S2). Moreover the substituents on C and E rings of 13*H*-benzo[*f*]chromeno[4,3-b][1,7]naphthyridin-5-ium chloride moieties have a key role in exhibiting dual topo I / IIα inhibitory activities. However, there was no direct correlation between the cytotoxic activities of tested compounds and their top I and IIα inhibitory activities.

2.2.3. Molecular docking study

The molecular docking simulations were performed to better understand the potential interaction modes of the compounds **48** and **52** with topo I and IIα. From the above studies, compound **48** inhibited both topo I and topo IIα. Fig. 5a shows the binding site of compound **48** with topo I where it intercalates into the single-strand cleavage site. There is no hydrogen bonding interactions between the compound **48** and topo I. Compound **48** have van der Waals interactions with residues Arg364, Pro431, and Asn722 and π- π stacking interactions with the stacked DNA bases. Fig. 6 depicts the binding site of compound **48** with topo IIα where it bound to the topo IIα DNA cleavage site where etoposide was situated. The benzo[*f*]chromeno[4,3-b][1,7]naphthyridine ring was stacked between the DNA bases of the cleavage site with π- π stacking interactions. Similar to the binding of topo I, there were no hydrogen bond interactions with topo IIα.

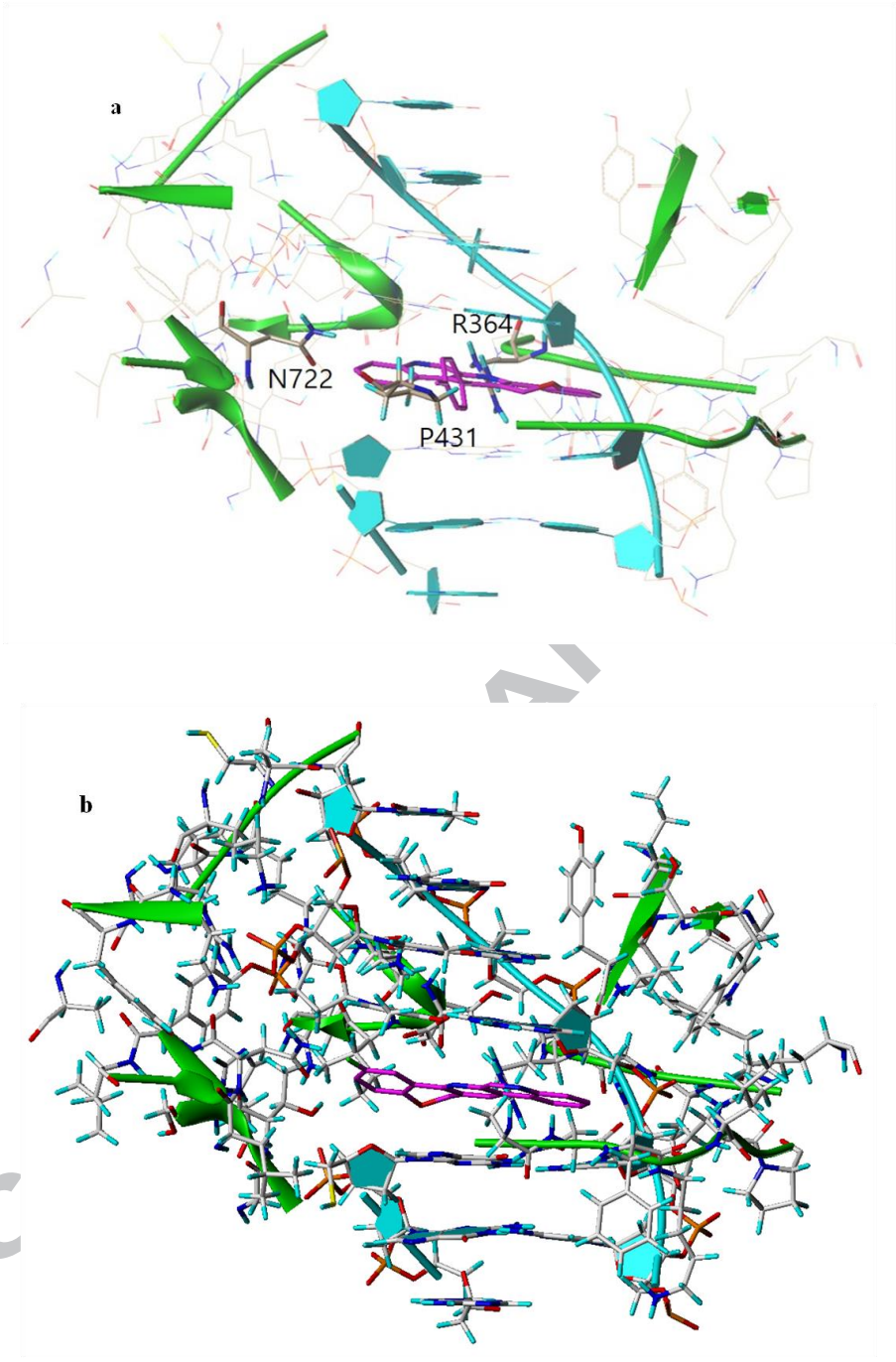

Fig 5. (**a**) Binding mode of the compound **48** with topo I. (**b**) binding mode of the compound **52** with topo I: Compounds **48**, **52** and the interacting residues of the receptor are depicted in capped sticks colored by atom types and taupe and magenta for carbon atoms of the receptor and compounds respectively. The DNA phosphate backbone and bases are displayed in cartoons in cyan and green.

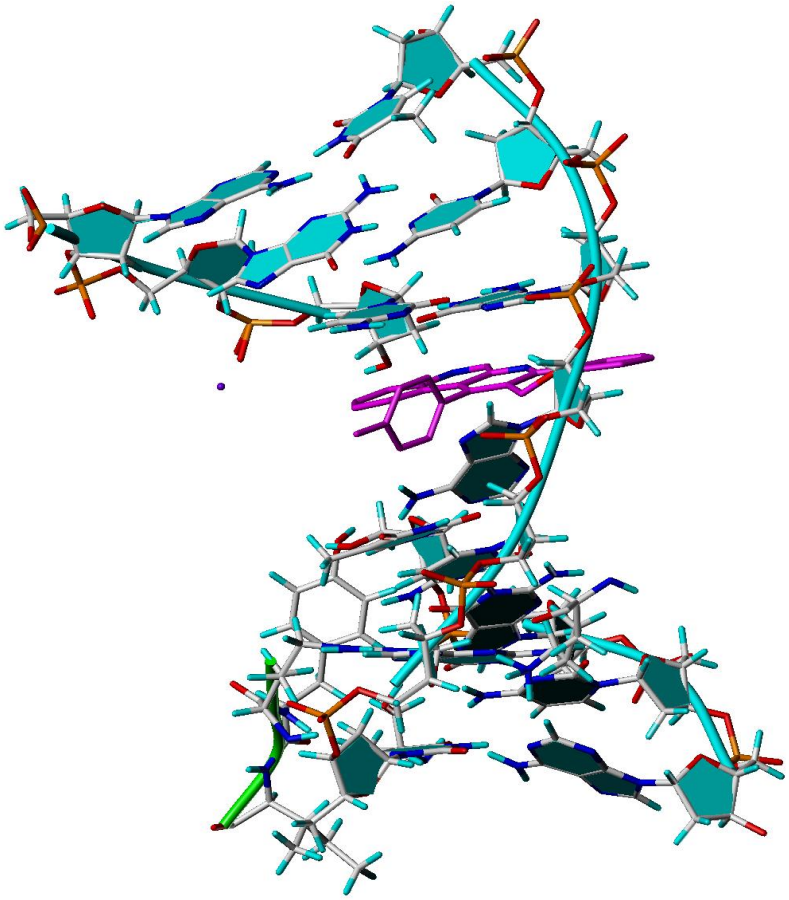

Fig 6. Binding mode of compound **48** with topo IIα: Compound **48** and the interacting residues of the receptor are shown in capped sticks colored by atom types and magenta for carbon atoms of the compound. The DNA phosphate backbone and bases are shown in cartoons in cyan and green.

Hence, it was obvious that the compound **48** acted as dual topo I/ IIα inhibitor. From the biological part, compound **52** inhibited topo I with excellent activity to the reference drug camptothecin. Fig. 5b reveals the binding site of the compound **52** with topo I where it was intercalated into the single-strand DNA cleavage site. There was no hydrogen bonding interaction between the compound **52** and topo I observed. The compound **52** have van der

Waals interactions with residues Arg364, Thr718, and Asn722. Hence, the compound **52** acted as topo I inhibitor.

3. Conclusion

Operationally simple, one-pot, regioselective and atom-economic synthetic pathway was successfully pioneered to the pentacyclic 13*H*-benzo[*f*]chromeno[4,3-b][1,7]naphthyridines (**21-39**) and 13*H*-benzo[*f*]chromeno[4,3-b][1,7]naphthyridin-5-ium chlorides (**40-53**). We have identified certain 13*H*-benzo[*f*]chromeno[4,3-b][1,7]naphthyridin-5-ium chlorides as a new type of dual topo I and topo IIα inhibitors with potential cytotoxic activities. In this study, we have screened novel 35 compounds against six different human cancer cell lines including lung cancer cell line (NCIH23), colon cancer cell line (HCT15), gastric cancer cell line (NUCG-3), renal cancer cell line (ACHN), prostate cancer cell line (PC-3), and breast cancer cell line (MDA-MB-231) with reference drug doxorubicin (ADR). Among all tested compounds, 8 compounds **28**, **30**, **34**, **35**, **46**, **48**, **52**, and **53** shown potential cytotoxicities against all tested human cancer cell lines. We have also evaluated the lead 8 cytotoxic agents against catalytic inhibitory action toward human topo I and topo IIα. As anticipated the compound **48** displayed dual topo I and topo IIα inhibition and compound **52** acts as potent topo I inhibitor. In particular at 20 μM concentrations, the compound **48** exhibited 1.25 times more potent topo IIα inhibitory activity than the positive control etoposide drug. The compound **52** exhibited 1.32 times more potent topo I inhibition than the reference drug camptothecin at 100 μM concentrations. The potency of these compounds dictates the importance of substituents on C and E rings of core motif of 13*H*-benzo[*f*]chromeno[4,3-b][1,7]naphthyridin-5-ium chlorides albeit the combination of tolyl group

at C ring with no substituents at E ring and no substituent on C ring and –F substituent on E ring being the most favorable. We have also carried out molecular docking studies with Sybyl X-2.1 using the default parameters to investigate the binding site of compounds **48** and **52** with human topo I and IIα respectively. The docking studies of the compounds **48** and **52** with topo I revealed they intercalated into the single-strand cleavage site where the compound **48** have van der Waals interactions with residues Arg364, Pro431, and Asn722 whereas the compound **52** with residues Arg364, Thr718, and Asn722. Both the compounds **48** and **52** have π- π stacking interactions with the stacked DNA bases. The docking studies of the compound **48** with topo IIα explored that the compound **48** bound to the topo IIα DNA cleavage site where etoposide was situated. The benzo[*f*]chromeno[4,3-*b*][1,7]naphthyridine ring of the compound **48** was stacked between the DNA bases of the cleavage site with π- π stacking interactions and there were no hydrogen bond interactions with topo IIα. Conclusively, the results of the present study provide noticeable rationale to design and synthesis of angularly fused molecules targeting dual topo I and topo IIα inhibition with potential wide spectrum of cytotoxic activities.

4. Experimental Section

All the reactions were carried out in oven dried glassware with freshly distilled dry solvents under anhydrous conditions unless otherwise indicated and all commercial chemicals were used as obtained. Evaporation of organic solutions was achieved by rotary evaporation with a water bath temperature below 40 ^{o}C. All the products obtained were purified by column chromatography using activated aluminum oxide basic (Brockmann I, 199443) and silica gel (100-200 mesh). Thin layer chromatography was performed on E Merck silica gel GF-254 pre-coated plates and aluminum oxide TLC plates; identification was performed under UV

illumination. Hexane was used as a co-eluent. ^{1}H and ^{13}C NMR were recorded in JEOL 400 and 101 MHz spectrometer respectively. The chemical shifts are reported in ppm downfield to TMS (δ = 0) for ^{1}H NMR and relative to the central $CDCl_3$ resonance (δ = 77.0) for ^{13}C NMR. Data are reported as follows: chemical shift in ppm (d), multiplicity (s = singlet, d = doublet, t = triplet, m = multiplet), coupling constant (Hz), and integration. High resolution mass spectra (HRMS, QTOF) recorded on LCQ Fleet-Thermo Scientifics.

4.1. General Procedure for the synthesis of 13H-benzo[f]chromeno[4,3-b][1,7]naphthyridines (21-39)

In an ace pressure tube or a round bottom flask equipped with a magnetic stirring bar, 1.0 equiv of 3-aminoquinoline, 0.5 equiv. of *O*-propargylated salicylaldehydes, 20 mol % of $Yb(OTf)_3$, 20 mol % of CuI, 0.5 equiv. of 4A^{o} molecular sieves and 5-10 mL of acetonitrile was added. Reaction mixture was stirred at reflux temperature. After completion of the reaction, as indicated by the Al_2O_3 TLC, dichloromethane (DCM, 10 mL) was added to the crude reaction mass and then filtered through Celite® pad and concentrated under the reduced pressure. Product was purified by column chromatography on activated aluminum oxide basic (Brockmann I, 199443) (eluent: hexanes/ethyl acetate) afforded the corresponding products (**21-39**).

4.1.1. 9-Bromo-14-methyl-13H-benzo[f]chromeno[4,3-b][1,7]naphthyridine (25)

Off-white solid (40.9%); R_f: 0.70 (eluent 2:3 Ethyl acetate: Hexanes); ^{1}H NMR (400 MHz, $CDCl_3$) δ 9.49 (s, 1H), 8.64 (dd, *J* = 13.6, 5.5 Hz, 2H), 8.27 (dd, *J* = 8.1, 1.4 Hz, 1H), 7.79 (ddd, *J* = 8.2, 7.1, 1.3 Hz, 1H), 7.70 (ddd, *J* = 8.5, 7.1, 1.6 Hz, 1H), 7.46 (dd, *J* = 8.7, 2.4 Hz, 1H), 6.91 (d, *J* = 8.6 Hz, 1H), 5.57 (s, 2H), 2.96 (s, 3H). ^{13}C NMR (101 MHz, $CDCl_3$) δ 164.31, 155.74, 150.18, 139.67, 134.80, 130.98, 128.77, 128.35, 128.14, 127.05, 126.82, 118.95, 115.34, 114.82,

113.54, 66.56, 19.42. HRMS m/z $[M+H]^+$ calculated for $C_{20}H_{14}N_2OBr$: 377.0289; Found: 377.0270.

4.1.2 9,11-Dichloro-14-methyl-13H-benzo[f]chromeno[4,3-b][1,7]naphthyridines (26)

Pale orange color solid; 57.2 % Yield; R_f: 0.50 (eluent 2:3 Ethyl acetate: Hexanes); ^1H NMR (500 MHz, $CDCl_3$) δ 9.50 (s, 1H), 8.69 (d, *J* = 7.8 Hz, 1H), 8.44 (d, *J* = 2.5 Hz, 1H), 8.30 (dd, *J* = 8.1, 1.4 Hz, 1H), 7.85 – 7.80 (m, 1H), 7.76 – 7.70 (m, 1H), 7.46 (d, *J* = 2.5 Hz, 1H), 5.70 (s, 2H), 2.99 (s, 3H). ^{13}C NMR (101 MHz, $CDCl_3$) δ 155.59, 150.92, 146.41, 145.56, 142.37, 139.92, 131.76, 130.98, 128.93, 128.14, 127.72, 127.59, 127.11, 126.80, 124.67, 123.99, 122.87, 67.05, 19.40. HRMS m/z $[M+H]^+$calculated for $C_{20}H_{13}N_2OCl_2$: 367.0404; Found: 367.0399.

4.1.3. 8-Bromo-11-methoxy-14-methyl-13H-benzo[f]chromeno[4,3-b][1,7]naphthyridine (27)

Off-white solid (41.5%); R_f: 0.45 (eluent 2:3 Ethyl acetate: Hexanes); ^1H NMR (400 MHz, $CDCl_3$) δ 9.56 (d, *J* = 22.9 Hz, 1H), 8.67 (d, *J* = 8.5 Hz, 1H), 8.27 (dt, *J* = 8.1, 1.6 Hz, 1H), 7.78 (ddd, *J* = 9.9, 5.6, 2.0 Hz, 1H), 7.69 (ddd, *J* = 8.5, 7.1, 1.5 Hz, 1H), 7.40 (d, *J* = 8.7 Hz, 1H), 5.50 (d, *J* = 3.3 Hz, 2H), 3.92 (d, *J* = 1.7 Hz, 3H), 3.00 (s, 3H). ^{13}C NMR (101 MHz, $CDCl_3$) δ 155.81, 155.50, 149.47, 148.43, 147.75, 145.70, 141.84, 139.12, 136.14, 130.94, 29.67, 128.92, 128.79, 127.00, 122.97, 114.78, 114.04, 110.78, 66.96, 56.41, 19.57. HRMS m/z $[M+H]^+$ calculated for $C_{21}H_{16}BrN_2O_2$: 407.0395; Found: 407.0385.

4.1.4. 14-(p-Tolyl)-13H-benzo[f]chromeno[4,3-b][1,7]naphthyridine (30)

Off-white solid (53.3%); R_f: 0.60 (eluent 2:3 Ethyl acetate: Hexanes); ^1H NMR (400 MHz, $CDCl_3$) δ 9.58 (s, 1H), 8.54 (dd, J = 1.6Hz, 1H), 8.17 (dd, J = 1.2, 1.3 Hz, 1H), 7.62-7.598 (m, 1H), 7.45 (d, J = 7.7 Hz, 2H), 7.41-7.33 (m, 2H), 7.22-7.18 (m, 4H), 6.99 (dd, J = 0.8 Hz, 1H)

5.08 (s, 2H); ^{13}C NMR (101 MHz, $CDCl_3$): δ 156.9, 155.5, 149.0, 145.3, 143.7, 142.5, 139.0, 134.5, 132.3, 130.8, 130.5, 128.3, 127.7, 126.6, 126.4, 125.8, 125.6, 123.9, 122.6, 117.0, 66.5, 21.5. HRMS m/z $[M+H]^+$calculated for $C_{26}H_{19}N_2O$: 375.1497; Found: 375.1490.

4.1.5. 9-Chloro-14-methyl-13H-benzo[f]chromeno[4,3-b][1,7]naphthyridine (31)

White solid (47.2%); R_f: 0.70 (eluent 1:4 Ethyl acetate: Hexanes); ^{1}H NMR (400 MHz, $CDCl_3$) δ 9.56 (s, 1H), 8.53 – 8.44 (m, 1H), 8.16 (d, J = 8.1 Hz, 1H), 7.60 (dd, J = 8.0, 7.1 Hz, 1H), 7.45 (d, J = 7.6 Hz, 2H), 7.37 (d, J = 8.6 Hz, 1H), 7.33 – 7.29 (m, 1H), 7.19 (t, J = 6.2 Hz, 3H), 6.95 – 6.87 (m, 1H), 5.06 (d, J = 0.8 Hz, 2H), 2.56 (s, 3H). ^{13}C NMR (101 MHz, $CDCl_3$) 155.46, 155.40, 147.86, 145.53, 144.02, 142.57, 139.20, 134.41, 132.05, 130.96, 130.66, 128.66, 128.05, 127.97, 127.76, 126.75, 126.51, 126.17, 125.34, 123.91, 123.84, 118.64, 66.71, 21.59. HRMS m/z $[M+H]^+$calculated for $C_{26}H_{18}ClN_2O$: 409.1107; Found: 409.1099 ($M+H^+$).

4.2. General Procedure for the synthesis of 13H-benzo[f]chromeno[4,3-b][1,7]naphthyridin-5-ium chlorides (40-56)

20 mg of 13*H*-benzo[f]chromeno[4,3-b][1,7]naphthyridines dissolved in 10 ml of MeOH at 0°C, to this reaction mixture added 1 ml of 37% HCl and stirred for 1 hour at 0°C. Then the reaction mixture continued to stir at room temperature for overnight. The reaction progress was monitored by TLC, and the hydrochloride salts of 13*H*-benzo[*f*]chromeno[4,3-*b*][1,7]naphthyridines **40-56** were obtained in almost quantitative yields by concentrating the reaction mixtures under reduced pressure.

4.2.1. 14-(p-tolyl)-13H-benzo[f]chromeno[4,3-b][1,7]naphthyridin-5-ium chloride (48)

Yellow color solid (Quantitative Yield); ^{1}H NMR (400 MHz, CD_3OD) δ 10.00 (s, 1H), 8.50 (dd, J = 7.9, 1.6 Hz, 1H), 8.26 (d, J = 8.4 Hz, 1H), 7.94 (ddd, J = 8.3, 7.0, 1.2 Hz, 1H), 7.66 – 7.43 (m, 5H), 7.36 – 7.29 (m, 2H), 7.26 – 7.16 (m, 1H), 7.00 (dd, J = 8.2, 0.7 Hz, 1H), 5.19 (s, 2H), 2.56 (s, 3H). ^{13}C NMR (101 MHz, CD_3OD) δ 157.68, 152.04, 151.41, 146.11, 144.39, 141.93, 140.93, 140.36, 138.94, 134.27, 133.74, 132.84, 131.24, 131.03, 129.58, 127.65, 127.18, 125.72, 125.21, 122.64, 121.99, 121.12, 117.63, 117.17, 66.33, 20.18.

4.2.2. 9-chloro-14-(p-tolyl)-13H-benzo[f]chromeno[4,3-b][1,7]naphthyridin-5-ium chloride (49)

Pale yellow color solid (Quantitative Yield); ^{1}H NMR (400 MHz, CD_3OD) δ 9.91 (s, 1H), 8.43 (d, *J* = 2.6 Hz, 1H), 8.21 (dd, *J* = 8.3, 1.0 Hz, 1H), 7.88 (ddd, *J* = 8.3, 7.0, 1.3 Hz, 1H), 7.60 – 7.52 (m, 3H), 7.51 – 7.45 (m, 1H), 7.41 (dd, *J* = 8.7, 2.6 Hz, 1H), 7.32 – 7.27 (m, 2H), 6.98 (d, *J* = 8.7 Hz, 1H), 5.18 (s, 2H), 2.54 (s, 3H). ^{13}C NMR (101 MHz, CD_3OD) δ 156.10, 151.88, 141.07, 140.98, 140.36, 133.25, 133.11, 132.85, 131.09, 131.02, 129.30, 127.76, 127.60, 127.54, 127.02, 125.21, 124.96, 123.03, 122.95, 122.53, 119.08, 118.98, 118.07, 117.88, 66.51, 20.18.

4.2.3. 9-fluoro-13H-benzo[f]chromeno[4,3-b][1,7]naphthyridin-5-ium chloride (52)

Beige color Solid (Quantitative Yield); ^{1}H NMR (400 MHz, CD_3OD) δ 9.99 (s, 1H), 9.28 (s, 1H), 9.08 – 8.98 (m, 1H), 8.38 – 8.29 (m, 1H), 8.22 – 8.09 (m, 3H), 7.27 (td, *J* = 8.4, 3.1 Hz, 1H), 7.12 (dd, *J* = 9.0, 4.5 Hz, 1H), 5.65 (d, *J* = 0.9 Hz, 2H). ^{13}C NMR (101 MHz, CD_3OD) δ 159.64, 157.27, 150.87, 148.68, 145.11, 143.92, 139.94, 135.32, 133.66, 132.34, 130.91, 127.67, 127.10, 124.13, 121.78, 120.16, 119.23, 110.74, 68.05.

4.2.4. 9-chloro-13H-benzo[f]chromeno[4,3-b][1,7]naphthyridin-5-ium chloride (53)

Acid green color Solid (Quantitative Yield); ^{1}H NMR (400 MHz, CD_3OD) δ 9.98 (s, 1H), 9.29 (s, 1H), 9.04 (dd, J = 7.7, 1.9 Hz, 1H), 8.48 (t, J = 2.9 Hz, 1H), 8.36 (dd, J = 7.5, 2.1 Hz, 1H), 8.18 – 8.14 (m, 1H), 7.50 (ddd, J = 15.2, 8.8, 2.5 Hz, 1H), 7.36 – 7.31 (m, 1H), 7.16 – 7.12 (m, 1H), 5.71 (d, J = 1.1 Hz, 2H). ^{13}C NMR (101 MHz, CD_3OD) δ 156.66, 151.19, 148.62, 145.59, 144.59, 133.19, 132.10, 130.66, 128.93, 127.82, 127.20, 126.92, 124.77, 124.08, 123.99, 122.49, 119.31, 114.17, 68.04.

4.2.5. 13H-benzo[f]chromeno[4,3-b][1,7]naphthyridin-5-ium chloride (55)

^{1}H NMR (400 MHz, CD_3OD) δ 9.98 (s, 1H), 9.27 (s, 1H), 9.14 – 8.95 (m, 1H), 8.49 (dd, *J* = 7.8, 1.6 Hz, 1H), 8.38 – 8.32 (m, 1H), 8.19 – 8.13 (m, 2H), 7.52 (ddd, *J* = 8.3, 7.4, 1.8 Hz, 1H), 7.26 – 7.16 (m, 1H), 7.10 (d, *J* = 8.1 Hz, 1H), 5.66 (d, *J* = 1.2 Hz, 2H). ^{13}C NMR (101 MHz, CD_3OD) δ 158.14, 152.77, 150.77, 135.36, 133.72, 132.63, 132.04, 130.71, 129.05, 128.40, 126.85, 125.48, 125.09, 124.05, 122.65, 122.06, 121.49, 117.46, 67.92, 48.29, 48.08, 47.87, 47.65, 47.44, 47.23, 47.01.

5. Materials and methods

5.1. Pharmacology

5.1.1. *In vitro cytotoxicity assay*

In vitro cytotoxicity assay was performed using the number of cells measured indirectly by the sulforhodamine B (SRB) method according to the NCI (USA) protocol. Cells were plated into a 96 well plate at a density of 2 103 cells per well. On the next day (day 0), the compounds of interest dissolved in DMSO/media were added in quadruplicate. The final concentration of

each compound ranged from 1 nM to 10 µM and the final concentration of DMSO was <0.1%. Seventy-two hours later, the cells were fixed with 10% trichloroacetic acid (TCA) overnight at 4°C, washed extensively with distilled water and dried in air. SRB solution (0.4% in 1% acetic acid) was then added to each well at room temperature for 1 h. The wells were washed with 1% acetic acid and bound dye was dissolved in 10 mM Tris. The absorbance was measured at 690 nm using a micro plate reader. The absorbance of the day 0 sample was subtracted from the absorbance of the day 3 sample.

5.1.2. In vitro assay for DNA topoisomerase I inhibition

The test compounds were dissolved in DMSO at 20 mM as stock solutions. The activity of DNA topo I was determined by assessing the relaxation of supercoiled DNA pBR322. The mixture of 100 ng of plasmid pBR322 DNA and 1 unit of recombinant human DNA topoisomerase I (TopoGEN INC., USA) was incubated without and with the prepared compounds at 37 ^{o}C for 30 min in the relaxation buffer (10 mM Tris-HCl (pH 7.9), 150 mM NaCl, 0.1% bovine serum albumin, 1 mM spermidine, 5% glycerol). The reaction in the final volume of 10 mL was terminated by adding 2.5 mL of the stop solution containing 5% sarcosyl, 0.0025% bromophenol blue and 25% glycerol. DNA samples were then electrophoresed on a 1% agarose gel at 15 V for 7 h with a running buffer of TAE. Gels were stained for 30 min in an aqueous solution of ethidium bromide (0.5 mg/mL). DNA bands were visualized by transillumination with UV light and were quantitated using AlphaImager™ (Alpha Innotech Corporation).

5.1.3. In vitro DNA topoisomerase-IIα inhibition assay

The mixture of 200 ng of super coiled pBR322 plasmid DNA and 4 units of human DNA topoisomerase-IIα (Sigma, USA) was incubated with the compounds [**28**, **30**, **34**, **35**, **46**, **48**, **52**,

53 and etoposide] in the assay buffer (10 mM Tris–HCl (pH 7.9) containing 50 mM NaCl, 5 mM $MgCl_2$, 1 mM EDTA, 1 mM ATP, and 15 µg/mL bovine serum albumin) for 30 min at 30 °C. The reaction in a final volume of 20 µL was terminated by the addition of 3 µL of 7 mM EDTA. Reaction products were analyzed on a 1% Agarose gel at 60 V for 1 h with a running buffer of TAE. Gels were stained for 30 min in an aqueous solution of ethidium bromide (0.5 µg/mL). DNA bands were visualized by transillumination with UV light.

6. Molecular docking

The structures of human Topo I and Topo IIα were generated based on their X-ray structures (PDB code: 1T8I [63] and 3QX3[64]) using SYBYL X-2.1.1 software package (Tripos, Inc. St. Louis, MO). Currently, the structure of topo IIβ complexed with etoposide and DNA is the only structure available with drug bound to topo II. Therefore, homology model of topo IIα was generated by Modeller (ver. 9.13) using 3QX3, x-ray crystal structure of human topo IIβ complexed with etoposide and DNA, as the template.[65] The sequences of human topo IIβ and topo IIα were aligned using ClustalW implemented in BioEdit program.[66] The homology model was generated using the aligned file. Etoposide and DNA from the template were transferred to the generated model. From the four homology models generated, the best model was chosen having the lowest DOPE score from the model assessment. The receptor protein structure was prepared by removing all the water molecules, ligands and adding hydrogen atoms. The coordinate file for the structure of compounds was constructed in Sybyl X-2.1.1 and energetically minimized using a Tripos force field with Gasteiger-Huckel charges. Docking of the compounds to topo I and Topo IIα were carried out using Sybyl X-2.1.1 with Surflex-Dock GeomX docking mode.

Acknowledgments

This research was supported by Basic Science Research Program through the National Research Foundation of Korea (NRF) funded by the Ministry of Education (NRF-2015R1D1A1A01058142), Korea Research Fellowship Program through the National Research Foundation of Korea (NRF) funded by the Ministry of Science, ICT and Future Planning (NRF-2016H1D3A1937140) and Medical Research Center Program (2017R1A5A2015541).

Supplementary data

Supplementary data associated with this article can be found, in the online version, at http://dx.doi.org/10.1016/j.bmc.

References

[1] M. Gellert, DNA topoisomerases, Annual review of biochemistry, 50 (1981) 879-910.

[2] H.P. Vosberg, Current Topics in Microbiology and Immunology, 114 (1985) 19-102.

[3] T.C. Boles, J.H. White, N.R. Cozzarelli, Structure of plectonemically supercoiled DNA, Journal of Molecular Biology, 213 (1990) 931-951.

[4] J.C. Wang, DNA topoisomerases, in: Annual Review of Biochemistry, 1996, pp. 635-692.

[5] J.J. Champoux, DNA topoisomerases: Structure, function, and mechanism, in: Annual Review of Biochemistry, 2001, pp. 369-413.

[6] F.H. Drake, J.P. Zimmerman, F.L. McCabe, H.F. Bartus, S.R. Per, D.M. Sullivan, W.E. Ross, M.R. Mattern, R.K. Johnson, S.T. Crooke, C.K. Mirabelli, Purification of topoisomerase II from

amsacrine-resistant P388 leukemia cells. Evidence for two forms of the enzyme, Journal of Biological Chemistry, 262 (1987) 16739-16747.

[7] F.H. Drake, G.A. Hofmann, H.F. Bartus, M.R. Mattern, S.T. Crooke, C.K. Mirabelli, Biochemical and Pharmacological Properties of p170 and p180 Forms of Topoisomerase II, Biochemistry, 28 (1989) 8154-8160.

[8] R.D. Woessner, M.R. Mattern, C.K. Mirabelli, R.K. Johnson, F.H. Drake, Proliferation- and cell cycle-dependent differences in expression of the 170 kilodalton and 180 kilodalton forms of topoisomerase II in NIH-3T3 cells, Cell growth & differentiation : the molecular biology journal of the American Association for Cancer Research, 2 (1991) 209-214.

[9] K.D. Corbett, J.M. Berger, Structure, molecular mechanisms, and evolutionary relationships in DNA topoisomerases, in: Annual Review of Biophysics and Biomolecular Structure, 2004, pp. 95-118.

[10] J. Dancey, E.A. Eisenhauer, Current perspectives on camptothecins in cancer treatment, British Journal of Cancer, 74 (1996) 327-338.

[11] N. Vicker, L. Burgess, I.S. Chuckowree, R. Dodd, A.J. Folkes, D.J. Hardick, T.C. Hancox, W. Miller, J. Milton, S. Sohal, S. Wang, S.P. Wren, P.A. Charlton, W. Dangerfield, C. Liddle, P. Mistry, A.J. Stewart, W.A. Denny, Novel angular benzophenazines: Dual topoisomerase I and topoisomerase II inhibitors as potential anticancer agents, Journal of Medicinal Chemistry, 45 (2002) 721-739.

[12] F. Arcamone, G. Cassinelli, G. Fantini, A. Grein, P. Orezzi, C. Pol, C. Spalla, Adriamycin, 14-hydroxydaunomycin, a new antitumor antibiotic from S. peucetius var. caesius, Biotechnology and Bioengineering, 67 (2000) 704-713.

[13] K.R. Hande, Topoisomerase II inhibitors, Update Cancer Ther. 1 (2006) 3-15.

[14] A.D. Marco, A.M. Casazza, R. Gambetta, R. Supino, F. Zunino, Relationship between Activity and Amino Sugar Stereochemistry of Daunorubicin and Adriamycin Derivatives, Cancer Research, 36 (1976) 1962-1966.

[15] F. Zunino, R. Gambetta, A. DiMarco, G. Luoni, A. Zaccara, Effects of the stereochemical configuration on the interaction of some daunomycin derivatives with DNA, Biochemical and Biophysical Research Communications, 69 (1976) 744-750.

[16] K.M. Tewey, T.C. Rowe, L. Yang, B.D. Halligan, L.F. Liu, Adriamycin-induced DNA damage mediated by mammalian DNA topoisomerase II, Science, 226 (1984) 466-468.

[17] E. Berman, A review of idarubicin in acute leukemia, ONCOLOGY, 7 (1993) 91-104.

[18] S.A. Feig, M.M. Ames, H.N. Sather, L. Steinherz, J.M. Reid, M. Trigg, T.W. Pendergrass, P. Warkentin, M. Gerber, M. Leonard, W.A. Bleyer, R.E. Harris, Comparison of idarubicin to daunomycin in a randomized multidrug treatment of childhood acute lymphoblastic leukemia at first bone marrow relapse: A report from the Children's Cancer Group, Medical and Pediatric Oncology, 27 (1996) 505-514.

[19] T.C. Rowe, G.L. Chen, Y.H. Hsiang, L.F. Liu, Dna damage by antitumor acridines mediated by mammalian dna topoisomerase II, Cancer Research, 46 (1986) 2021-2026.

[20] H.Y. Yap, G.R. Blumenschein, B.C. Barnes, F.C. Schell, G.P. Bodey, B.S. Yap, Bisantrene, an Active New Drug in the Treatment of Metastatic Breast Cancer, Cancer Research, 43 (1983) 1402-1404.

[21] K.M. Tewey, G.L. Chen, E.M. Nelson, L.F. Liu, Intercalative antitumor drugs interfere with the breakage-reunion reaction of mammalian DNA topoisomerase II, Journal of Biological Chemistry, 259 (1984) 9182-9187.

[22] W. Ross, B. Glisson, J. Yalowich, T. Rowe, L. Liu, Role of Topoisomerase II in Mediating Epipodophyllotoxin-induced DNA Cleavage, Cancer Research, 44 (1984) 5857-5860.

[23] G.J. Atwell, G.W. Rewcastle, B.C. Baguley, W.A. Denny, Potential Antitumor Agents. 50. In Vivo Solid-Tumor Activity of Derivatives of N-[2-(Dimethylamino)ethyl]acridine-4-carboxamide, Journal of Medicinal Chemistry, 30 (1987) 664-669.

[24] J.M. Fortune, L. Velea, D.E. Graves, T. Utsugi, Y. Yamada, N. Osheroff, DNA topoisomerases as targets for the anticancer drug TAS-103: DNA interactions and topoisomerase catalytic inhibition, Biochemistry, 38 (1999) 15580-15586.

[25] C.H. Nguyen, E. Bisagni, J.M. Lhoste, F. Lavelle, M.C. Bissery, Synthesis and Antitumor Activity of l-[[(Dialkylamino)alkyl]amino]-4-methyl-5H-pyrido[4,3-b]benzo[e]- and -benzo[g])indoles. A New Class of Antineoplastic Agents, Journal of Medicinal Chemistry, 33 (1990) 1519-1528.

[26] D. Perrin, B. Van Hille, J.M. Barret, A. Kruczynski, C. Etiévant, T. Imbert, B.T. Hill, F 11782, a novel epipodophylloid non-intercalating dual catalytic inhibitor of topoisomerases I and II with an original mechanism of action, Biochemical Pharmacology, 59 (2000) 807-819.

[27] A.A. Adjei, M. Charron, E.K. Rowinsky, P.A. Svingen, J. Miller, J.M. Reid, J. Sebolt-Leopold, M.M. Ames, S.H. Kaufmann, Effect of Pyrazoloacridine (NSC 366140) on DNA topoisomerases I and II, Clinical Cancer Research, 4 (1998) 683-691.

[28] S. Salerno, F. Da Settimo, S. Taliani, F. Simorini, C. La Motta, G. Fornaciari, A.M. Marini, Recent advances in the development of dual topoisomerase I and II inhibitors as anticancer drugs, Current Medicinal Chemistry, 17 (2010) 4270-4290.

[29] W.A. Denny, B.C. Baguley, Dual topoisomerase I/II inhibitors in cancer therapy, Current topics in medicinal chemistry, 3 (2003) 339-353.

[30] N. Vicker, L. Burgess, I.S. Chuckowree, R. Dodd, A.J. Folkes, D.J. Hardick, T.C. Hancox, W. Miller, J. Milton, S. Sohal, S. Wang, S.P. Wren, P.A. Charlton, W. Dangerfield, C. Liddle, P. Mistry, A.J. Stewart, W.A. Denny, Novel angular benzophenazines: Dual topoisomerase I and topoisomerase II inhibitors as potential anticancer agents, Journal of Medicinal Chemistry, 45 (2002) 721-739.

[31] C.H. Tseng, C.C. Tzeng, C.L. Yang, P.J. Lu, H.L. Chen, H.Y. Li, Y.C. Chuang, C.N. Yang, Y.L. Chen, Synthesis and antiproliferative evaluation of certain indeno[1,2-c] quinoline derivatives. Part 2, Journal of Medicinal Chemistry, 53 (2010) 6164-6179.

[32] R. Karki, P. Thapa, H.Y. Yoo, T.M. Kadayat, P.-H. Park, Y. Na, E. Lee, K.-H. Jeon, W.-J. Cho, H. Choi, Y. Kwon, E.-S. Lee, Dihydroxylated 2,4,6-triphenyl pyridines: Synthesis, topoisomerase I and II inhibitory activity, cytotoxicity, and structure–activity relationship study, European Journal of Medicinal Chemistry, 49 (2012) 219-228.

[33] M. Abdel-Aziz, S.-E. Park, G.E.-D.A.A. Abuo-Rahma, M.A. Sayed, Y. Kwon, Novel N-4-piperazinyl-ciprofloxacin-chalcone hybrids: Synthesis, physicochemical properties, anticancer and topoisomerase I and II inhibitory activity, European Journal of Medicinal Chemistry, 69 (2013) 427-438.

[34] L. Dalla Via, G. Marzaro, A. Ferrarese, O. Gia, A. Chilin, Pyrroloquinolinone-based dual topoisomerase I/II inhibitor, European Journal of Medicinal Chemistry, 77 (2014) 103-109.

[35] B.-L. Yao, Y.-W. Mai, S.-B. Chen, H.-T. Xie, P.-F. Yao, T.-M. Ou, J.-H. Tan, H.-G. Wang, D. Li, S.-L. Huang, L.-Q. Gu, Z.-S. Huang, Design, synthesis and biological evaluation of novel 7-alkylamino substituted benzo[a]phenazin derivatives as dual topoisomerase I/II inhibitors, European Journal of Medicinal Chemistry, 92 (2015) 540-553.

[36] R. Karki, K.-Y. Jun, T.M. Kadayat, S. Shin, T.B. Thapa Magar, G. Bist, A. Shrestha, Y. Na, Y. Kwon, E.-S. Lee, A new series of 2-phenol-4-aryl-6-chlorophenyl pyridine derivatives as dual topoisomerase I/II inhibitors: Synthesis, biological evaluation and 3D-QSAR study, European Journal of Medicinal Chemistry, 113 (2016) 228-245.

[37] H. Lee, S.-I. Lee, J. Cho, S.U. Choi, S.-I. Yang, Synthesis and in vitro evaluation of 1,8-diazaanthraquinones bearing 3-dialkylaminomethyl or 3-(N-alkyl- or N-aryl)carbamoyloxymethyl substituent, European Journal of Medicinal Chemistry, 38 (2003) 695-702.

[38] S.K. Arepalli, B. Park, K. Lee, H. Jo, K.-Y. Jun, Y. Kwon, J.-S. Kang, J.-K. Jung, H. Lee, Design, synthesis and biological evaluation of 1,3-diphenylbenzo[f][1,7]naphthyrdines, Bioorganic & Medicinal Chemistry, 25 (2017) 5586-5597.

[39] R. Pratap, V.J. Ram, Natural and Synthetic Chromenes, Fused Chromenes, and Versatility of Dihydrobenzo[h]chromenes in Organic Synthesis, Chemical Reviews, 114 (2014) 10476-10526.

[40] A. Bizarro, D. Sousa, T.R. Lima, L. Musso, R. Cincinelli, V. Zuco, M. De Cesare, S. Dallavalle, H.M. Vasconcelos, Synthesis and Evaluation of the Tumor Cell Growth Inhibitory Potential of New Putative HSP90 Inhibitors, Molecules, 23 (2018).

[41] M.I. Hegab, A.S.M. Abdel-Fattah, N.M. Yousef, H.F. Nour, A.M. Mostafa, M. Ellithey, Synthesis, X-ray structure, and pharmacological activity of some 6,6-disubstituted chromeno[4,3-b]- and chromeno-[3,4-c]-quinolines, Archiv der Pharmazie, 340 (2007) 396-403.

[42] R. Miri, R. Motamedi, M.R. Rezaei, O. Firuzi, A. Javidnia, A. Shafiee, Design, synthesis and evaluation of cytotoxicity of novel chromeno[4,3-b]quinoline derivatives, Archiv der Pharmazie, 344 (2011) 111-118.

[43] N. Mulakayala, D. Rambabu, M.R. Raja, M.C. Chaitanya, C.S. Kumar, A.M. Kalle, G. Rama Krishna, C. Malla Reddy, M.V. Basaveswara Rao, M. Pal, Ultrasound mediated catalyst free synthesis of 6H-1-benzopyrano[4,3-b] quinolin-6-ones leading to novel quinoline derivatives: Their evaluation as potential anti-cancer agents, Bioorganic and Medicinal Chemistry, 20 (2012) 759-768.

[44] U. Thapa, P. Thapa, R. Karki, M. Yun, J.H. Choi, Y. Jahng, E. Lee, K.-H. Jeon, Y. Na, E.-M. Ha, W.-J. Cho, Y. Kwon, E.-S. Lee, Synthesis of 2,4-diaryl chromenopyridines and evaluation of their topoisomerase I and II inhibitory activity, cytotoxicity, and structure–activity relationship, European Journal of Medicinal Chemistry, 46 (2011) 3201-3209.

[45] P. Thapa, E.S. Lee, 2,4-diaryl-5H-chromeno [4,3-b]pyridines: Synthesis, topoisomerase i and II inhibitory activity, and cytotoxicity, Bulletin of the Korean Chemical Society, 33 (2012) 3103-3106.

[46] S. Park, T.M. Kadayat, K.-Y. Jun, T.B. Thapa Magar, G. Bist, A. Shrestha, E.-S. Lee, Y. Kwon, Novel 2-aryl-4-(4′-hydroxyphenyl)-5H-indeno[1,2-b]pyridines as potent DNA non-intercalative topoisomerase catalytic inhibitors, European Journal of Medicinal Chemistry, 125 (2017) 14-28.

[47] B.-L. Yao, Y.-W. Mai, S.-B. Chen, H.-T. Xie, P.-F. Yao, T.-M. Ou, J.-H. Tan, H.-G. Wang, D. Li, S.-L. Huang, L.-Q. Gu, Z.-S. Huang, Design, synthesis and biological evaluation of novel 7-alkylamino substituted benzo[a]phenazin derivatives as dual topoisomerase I/II inhibitors, European Journal of Medicinal Chemistry, 92 (2015) 540-553.

[48] H.-B. Kwon, C. Park, K.-H. Jeon, E. Lee, S.-E. Park, K.-Y. Jun, T.M. Kadayat, P. Thapa, R. Karki, Y. Na, M.S. Park, S.B. Rho, E.-S. Lee, Y. Kwon, A Series of Novel Terpyridine-Skeleton Molecule Derivants Inhibit Tumor Growth and Metastasis by Targeting Topoisomerases, Journal of Medicinal Chemistry, 58 (2015) 1100-1122.

[49] S. Park, T.B. Thapa Magar, T.M. Kadayat, H.J. Lee, G. Bist, A. Shrestha, E.-S. Lee, Y. Kwon, Rational design, synthesis, and evaluation of novel 2,4-Chloro- and Hydroxy-Substituted diphenyl Benzofuro[3,2-b]Pyridines: Non-intercalative catalytic topoisomerase I and II dual inhibitor, European Journal of Medicinal Chemistry, 127 (2017) 318-333.

[50] P. Thapa, R. Karki, H.Y. Yoo, P.-H. Park, E. Lee, K.-H. Jeon, Y. Na, W.-J. Cho, Y. Kwon, E.-S. Lee, 2,4-Diaryl-5,6-dihydro-1,10-phenanthroline and 2,4-diaryl-5,6-dihydrothieno[2,3-h]

quinoline derivatives for topoisomerase I and II inhibitory activity, cytotoxicity, and structure–activity relationship study, Bioorganic Chemistry, 40 (2012) 67-78.

[51] P. Thapa, E.S. Lee, 2,4-diaryl-5,6-dihydro-1,10-phenanthrolines with furyl or thienyl moiety at 4-position: Synthesis, topoisomerase I and II inhibitory activity, and cytotoxicity, Bulletin of the Korean Chemical Society, 33 (2012) 1769-1772.

[52] X. Xiao, M. Cushman, An ab initio quantum mechanics calculation that correlates with ligand orientation and DNA cleavage site selectivity in camptothecin-DNA-topoisomerase I ternary cleavage complexes, Journal of the American Chemical Society, 127 (2005) 9960-9961.

[53] Y. Fan, J.N. Weinstein, K.W. Kohn, L.M. Shi, Y. Pommier, Molecular Modeling Studies of the DNA−Topoisomerase I Ternary Cleavable Complex with Camptothecin, Journal of Medicinal Chemistry, 41 (1998) 2216-2226.

[54] M.R. Redinbo, L. Stewart, P. Kuhn, J.J. Champoux, W.G.J. Hol, Crystal structures of human topoisomerase I in covalent and noncovalent complexes with DNA, Science, 279 (1998) 1504-1513.

[55] J.E. Kerrigan, D.S. Pilch, A Structural Model for the Ternary Cleavable Complex Formed between Human Topoisomerase I, DNA, and Camptothecin, Biochemistry, 40 (2001) 9792-9798.

[56] S.K. Arepalli, Y. Choi, K. Lee, J.-S. Kang, J.-K. Jung, H. Lee, Transition-metal-free, atom-economical cascade synthesis of novel 2-sulfonated-benzo[f][1,7]naphthyridines and their cytotoxic activities, Tetrahedron, 74 (2018) 1646-1654.

[57] S.K. Arepalli, B. Park, J.K. Jung, K. Lee, H. Lee, A facile one-pot regioselective synthesis of functionalized novel benzo[f]chromeno[4,3-b][1,7]naphthyridines and

benzo[f][1,7]naphthyridines via an imino Diels-Alder reaction, Tetrahedron Letters, 58 (2017) 449-454.

[58] H. Jo, M. Choi, A.S. Kumar, Y. Jung, S. Kim, J. Yun, J.S. Kang, Y. Kim, S.B. Han, J.K. Jung, J. Cho, K. Lee, J.H. Kwak, H. Lee, Development of Novel 1,2,3,4-Tetrahydroquinoline Scaffolds as Potent NF-κB Inhibitors and Cytotoxic Agents, ACS Medicinal Chemistry Letters, 7 (2016) 385-390.

[59] S.K. Arepalli, M. Choi, J.K. Jung, H. Lee, Novel NF-κB inhibitors: A patent review (2011-2014), Expert Opinion on Therapeutic Patents, 25 (2015) 319-334.

[60] M. Choi, H. Jo, H.J. Park, A. Sateesh Kumar, J. Lee, J. Yun, Y. Kim, S.B. Han, J.K. Jung, J. Cho, K. Lee, J.H. Kwak, H. Lee, Design, synthesis, and biological evaluation of benzofuran- and 2,3-dihydrobenzofuran-2-carboxylic acid N-(substituted)phenylamide derivatives as anticancer agents and inhibitors of NF-κB, Bioorganic and Medicinal Chemistry Letters, 25 (2015) 2545-2549.

[61] M. Choi, Y.S. Hwang, A.S. Kumar, H. Jo, Y. Jeong, Y. Oh, J. Lee, J. Yun, Y. Kim, S.B. Han, J.K. Jung, J. Cho, H. Lee, Design and synthesis of 3,4-dihydro-2H-benzo[h]chromene derivatives as potential NF-κB inhibitors, Bioorganic and Medicinal Chemistry Letters, 24 (2014) 2404-2407.

[62] A.F.M.M. Rahman, S.-E. Park, A.A. Kadi, Y. Kwon, Fluorescein Hydrazones as Novel Nonintercalative Topoisomerase Catalytic Inhibitors with Low DNA Toxicity, Journal of Medicinal Chemistry, 57 (2014) 9139-9151.

[63] B.L. Staker, M.D. Feese, M. Cushman, Y. Pommier, D. Zembower, L. Stewart, A.B. Burgin, Structures of three classes of anticancer agents bound to the human topoisomerase I-DNA covalent complex, Journal of Medicinal Chemistry, 48 (2005) 2336-2345.

[64] C.C. Wu, T.K. Li, L. Farh, L.Y. Lin, T.S. Lin, Y.J. Yu, T.J. Yen, C.W. Chiang, N.L. Chan, Structural basis of type II topoisomerase inhibition by the anticancer drug etoposide, Science, 333 (2011) 459-462.

[65] A. Sali, T.L. Blundell, Comparative protein modelling by satisfaction of spatial restraints. J of Molelcular Biology, 234 (1993) 779-815.

[66] T.A. Hall, BioEdit: a user-friendly biological sequence alignment editor and analysis program for Windows 95/98/NT Nucleic Acids Symposium Series, 41 (1999) 95-98.

Highlights:

- Novel thirty-five angularly fused heterocycles were designed, synthesized and evaluated.
- Eight compounds displayed significant cytotoxic activities against all tested human cancer cell lines
- The compound **48** exhibited dual human Topoisomerase I and IIα inhibition
- The compound **52** exhibited 1.32 times more potent topo I inhibition than camptothecin
- Molecular docking explored the binding sites of the compounds **48** and **52** with Topo I and IIα.

Graphical Abstract